Author Manuscript

Author Manuscript

Author Manuscript

Author Manuscript

HHS Public Access

Author manuscript

*Glia*. Author manuscript; available in PMC 2019 October 01.

Published in final edited form as:

*Glia*. 2018 October ; 66(10): 2094–2107. doi:10.1002/glia.23463.

# Astrocytes and neurons produce distinct types of polyglucosan bodies in Lafora Disease

**Elisabet Augé**[1,2], **Carme Pelegrí**[1,2,3], **Gemma Manich**[1], **Itsaso Cabezón**[1,2], **Joan J. Guinovart**[4,5,6], **Jordi Duran**[4,5,*], and **Jordi Vilaplana**[1,2,3,*]

[1]Secció de Fisiologia, Departament de Bioquímica i Fisiologia, Universitat de Barcelona, Barcelona, Spain

[2]Institut de Neurociències, Universitat de Barcelona, Barcelona, Spain

[3]Centros de Biomedicina en Red de Enfermedades Neurodegenerativas (CIBERNED), Spain

[4]Institute for Research in Biomedicine (IRB Barcelona), The Barcelona Institute of Science and Technology, Barcelona, Spain

[5]Centro de Investigación Biomédica en Red de Diabetes y Enfermedades Metabólicas Asociadas (CIBERDEM), Spain

[6]Departament de Bioquímica i Biomedicina Molecular, Universitat de Barcelona, Barcelona, Spain

## Abstract

Lafora disease (LD), the most devastating adolescence-onset epilepsy, is caused by mutations in the *EPM2A* or *EPM2B* genes, which encode the proteins laforin and malin, respectively. Loss of function of one of these proteins, which are involved in the regulation of glycogen synthesis, induces the accumulation of polyglucosan bodies (PGBs)—known as Lafora bodies (LBs) and associated with neurons—in the brain. Ageing and some neurodegenerative conditions lead to the appearance of another type of PGB called corpora amylacea, which are associated with astrocytes and contain neo-epitopes that can be recognized by natural antibodies. Here we studied the PGBs in the cerebral cortex and hippocampus of malin knockout mice, a mouse model of LD. These animals presented not only LBs associated with neurons but also a significant number of PGBs associated with astrocytes. These astrocytic PGBs were also increased in mice from senescence-accelerated mouse-prone 8 (SAMP8) strain and mice with overexpression of Protein Targeting to Glycogen ($PTG^{OE}$), indicating that they are not exclusive of LD. The astrocytic PGBs, but not neuronal LBs, contained neo-epitopes that are recognized by natural antibodies. The astrocytic PGBs appeared predominantly in the hippocampus but were also present in some cortical brain regions, while neuronal LBs were found mainly in the brain cortex and the pyramidal layer of

**Corresponding authors**: Dr. Jordi Duran, Institute for Research in Biomedicine (IRB Barcelona), The Barcelona Institute of Science and Technology, Carrer de Baldiri Reixac 10-12, 08028 Barcelona, Spain. Tel. (+34) 93 4037162 jordi.duran@irbbarcelona.org, Dr. Jordi Vilaplana, Secció de Fisiologia, Departament de Bioquímica i Fisiologia, Facultat de Farmàcia i Ciències de l'Alimentació, Av. Joan XXIII 27-31, 08028 Barcelona, Spain. Tel. (+34) 93 4024505. vilaplana@ub.edu.

*Jordi Duran, Jordi Vilaplana contributed equally to these work

**Conflict of interest**: The authors declare no competing financial interests

Author Manuscript Author Manuscript Author Manuscript Author Manuscript

hippocampal regions CA2 and CA3. Our results indicate that astrocytes, contrary to current belief, are involved in the etiopathogenesis of LD.

## Graphical abstract

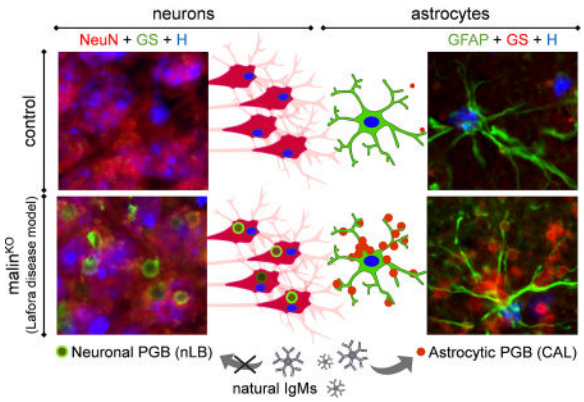


### Keywords

Lafora body; *Corpora amylacea*; Malin; Neo-epitope; Natural antibody

## Introduction

The term “polyglucosan bodies” (PGBs) refers to complex molecular aggregates composed of relatively large glucose polymers reaching diameters of tens of micrometres. PGBs have been reported in the central nervous system, but also in other organs and tissues, such as heart, skeletal muscle and liver (Cavanagh, 1999). While these aggregates have been described in humans and other species, they have been most widely studied in mammals. Various forms of PGB are linked to specific diseases. For example, *corpora amylacea* (CA) accumulate in the human brain during normal aging and to a greater extent in several neurodegenerative conditions, including Alzheimer’s, Parkinson’s, Huntington’s and Pick’s diseases (Pirici and Margaritescu, 2014; Rohn, 2015). Although human brain CA are formed mainly by aggregates of polymerized glucose, the presence of waste elements is a recurrent feature of these structures. This observation suggests that that they are involved in the trapping and sequestration of potentially hazardous products (Cavanagh, 1999; Pirici and Margaritescu, 2014; Rohn, 2015). We recently demonstrated that brain CA contain a number of neo-epitopes (Augé et al., 2017). The neo-epitopes are specific epitopes that are not present in healthy brain structures but appear in situations of cellular stress and tissue damage (Binder, 2010). We also found that the neo-epitopes present in CA are recognized by natural IgM antibodies, thus revealing the potential role of the natural immune system in CA removal (Augé et al., 2017). That study of the interaction between CA and the natural immune system was based on previous findings obtained in mice (Manich et al., 2015; Manich et al., 2016). In the same way in which CA accumulate with age in the human brain, aging in the mouse brain leads to the progressive appearance of PGBs, these generally referred to as “PAS granules” because of their positive staining with Periodic acid-Schiff (PAS). Given that the term “PAS granules” used to describe these mouse inclusions leads to

Author Manuscript Author Manuscript Author Manuscript Author Manuscript

misinterpretation because all PGBs are stained by PAS, in the present study we refer to them as CA-like (CAL) granules, because of their similarities to the CA of the human brain. CAL granules are present in a wide range of mouse strains, but they are particularly abundant in the senescence-accelerated mouse prone 8 (SAMP8) model (Manich et al., 2016). The SAMP8 model is a non-genetically modified strain of mice with a characteristic accelerated aging process that shares characteristics with aged humans, such as a reduced lifespan, lordosis, hair loss, and reduced physical activity (Hamamoto et al., 1984; Takeda et al., 1994). In these animals, CAL granules appear in various regions of the brain as early as three months of age, and their number increases faster than in other strains (Del Valle et al., 2010; Jucker et al., 1994a, 1994b; Kuo et al., 1996). CAL granules arise from a degenerative process that affects astrocytic processes and their surrounding neuropil, and the granules are organized into clusters, each one associated with a specific astrocyte (Manich et al., 2014a). As observed for CA, some neo-epitopes appear during CAL granule formation (Manich et al., 2014b), and they are recognized by natural IgMs (Manich et al., 2015; Manich et al., 2016). We also found that many commercial antibodies are contaminated with natural IgMs, thus leading to false positive staining in immunohistochemical studies of CAL granules in mice (Manich et al., 2014b; Manich et al., 2016) and of CA in the human brain (Augé et al., 2017). These false positive immunostainings contribute to explaining the controversial results of research addressing CA and CAL granules and reveal the need to re-examine many of the immunohistochemical studies carried out to date.

Human diseases like Adult Polyglucosan Body Disease (APBD) and Lafora disease (LD) are also characterized by the accumulation of PGBs in the brain (Cavanagh, 1999; Pirici and Margaritescu, 2014). LD, the most devastating form of adolescence-onset epilepsy, is perhaps the most striking example of the accumulation of PBGs in this organ. These PGBs are referred to as Lafora bodies (LBs). LBs are formed by abnormal poorly branched glycogen that aggregates and amasses into large neuronal inclusions over time (Duran and Guinovart, 2015). LB deposition in the brain leads to the onset and inexorable worsening of neurodegeneration and epilepsy, leading to death by early adulthood (Cavanagh, 1999; Minassian, 2001; Pirici and Margaritescu, 2014). LD is an autosomal recessive myoclonus epilepsy caused by mutations in one of the following two genes: *EPM2A*, which encodes laforin, a dual-specificity protein phosphatase with a functional carbohydrate-binding domain (Minassian et al., 1998; Serratosa et al., 1999); and *EPM2B*, which encodes malin, an E3 ubiquitin ligase (Chan et al., 2003). Individuals with mutations in *EPM2A* or *EPM2B* are neurologically and histologically indistinguishable. Laforin can function as a glucan phosphatase, removing the phosphate groups attached to glycogen (Tagliabracci et al., 2007). This finding, along with the hyperphosphorylation of glycogen in laforin knockout mice (laforin$^{KO}$), led to the hypothesis that elevated levels of phosphate esters cause the abnormal glycogen structure and trigger LB formation (Roach, 2015; Tagliabracci et al., 2008). However, the phosphatase activity of laforin does not appear to be required to prevent the disease (Gayarre et al., 2014), and glycogen hyperphosphorylation does not cause the formation of LBs (Nitschke et al., 2017). Also, there is evidence that laforin and malin form a complex, and these proteins have been described to regulate glycogen accumulation through proteasome-dependent control of glycogen-related proteins, such as Protein Targeting to Glycogen (PTG) (Vilchez et al., 2007; Worby et al., 2008), Muscle Glycogen

Author Manuscript Author Manuscript Author Manuscript Author Manuscript

Synthase (MGS) (Vilchez et al., 2007) and glycogen debranching enzyme (Cheng et al., 2007). In addition, it has been reported that laforin and malin are involved in the clearance of misfolded proteins through the ubiquitin–proteasome system (Garyali et al., 2009; Rao et al., 2010) and in the autophagy degradation pathway (Aguado et al., 2010; Criado et al., 2012; Knecht et al., 2010; Puri et al., 2012). In previous studies, we generated a malin knockout mouse (malin$^{KO}$) as a model of LD, and combined it with a mouse with a specific deletion of MGS in the brain (MGS$^{KO}$) (Duran et al., 2013), to generate a double malin$^{KO}$+MGS$^{KO}$ mouse. We observed that malin$^{KO}$ animals accumulate LBs in the brain and other tissues and show neurodegeneration and functional impairments, including disrupted autophagy (Vallés-Ortega et al., 2011; Duran et al., 2014). The malin$^{KO}$+MGS$^{KO}$ mouse did not show the accumulation of LBs, neurodegeneration or autophagy impairment seen in the malin$^{KO}$ animals (Duran et al., 2014), thereby suggesting that all these defects are a consequence of glycogen accumulation. Moreover, mice overexpressing PTG (PTG$^{OE}$), in which GS activity is increased, present high accumulation of PGBs in the brain (Duran et al., 2014). It is remarkable that although accumulations of CA have been described in several neurodegenerative conditions, including Alzheimer's, Parkinson's, Huntington's and Pick's diseases, the studies of PGBs in LD are centered in neuronal LBs, and the presence of astrocytic CAL granules in mouse models of LD has not yet been studied.

In this study, we explore, on the one hand, the presence of astrocytic CAL granules in the brain of a mouse model of LD, with the aim to determine whether this disease is characterized not only by altered neuronal function but also by the involvement of astrocytes. On the other hand, we address whether the LBs present in LD contain neo-epitopes that are recognized by natural IgMs. To this end, we used malin$^{KO}$ mice and compared them with mice from other strains or models, such as SAMP8, MGS$^{KO}$ and PTG$^{OE}$ animals.

## Materials and methods

### Mice

Malin$^{KO}$, PTG$^{OE}$ and MGS$^{KO}$ mice were generated as previously described (Duran et al., 2014). After weaning, at 3 weeks of age, tail clippings were taken for genotyping by qPCR (performed by Transnetyx). Wild-type littermates from the different colonies were used as controls. SAMP8 mice were obtained from the *Servei d'Estabulari de la Facultat de Farmàcia i Ciències de l'Alimentació* (*Universitat de Barcelona*). All procedures were approved by the Barcelona Science Park's Animal Experimentation Committee and the Ethical Committee for Animal Experimentation of the *Universitat de Barcelona* and were carried out in accordance with the European Community Council Directive and National Institutes of Health guidelines for the care and use of laboratory animals. Mice were maintained on a 12/12 h light/dark cycle under standard room temperature (RT) and allowed free access to a commercial chow diet and water throughout the study. All experiments were performed with animals aged between 60 and 80 weeks (n=4 for each experimental group).

Author Manuscript Author Manuscript Author Manuscript Author Manuscript

### Brain processing

Frozen or paraffin-embedded brain sections were used. To obtain frozen sections, animals were anesthetized intraperitoneally with sodium pentobarbital (80 mg/kg) and given an intracardiac gravity-dependent perfusion of 50 mL of saline solution. Brains were dissected and frozen by immersion in isopentane and then chilled in dry ice. Frozen brains were then cut at the coronal plane into 20-µm-thick sections on a cryostat (Leica Microsystems, Germany) at −22°C and placed on slides. Coronal sections from bregma around −2.30 were selected, and the studies were performed considering the hippocampus and the cortex located between the retrosplenial granular region and the primary somatosensory cortex as the regions of interest. Sections were fixed with acetone for 10 min at 4°C and frozen at −20°C. To obtain paraffin-embedded sections (used in $PTG^{OE}$ mice), animals were perfused transcardially with phosphate-buffered saline (PBS) containing 4% of paraformaldehyde (PF). Brains were removed, postfixed overnight with PBS 4% PF, and embedded in paraffin. Paraffin sections were then cut to a thickness of 5 µm in a microtome.

### PAS staining

Frozen sections were stained with PAS following the standard procedure. Briefly, sections were fixed for 10 min in Carnoy's solution (60% ethanol, 30% chloroform and 10% glacial acetic acid). The slides were then pretreated for 10 min with 0.25% periodic acid (19324-50, Electron Microscopy Sciences) in distilled water, followed by a washing step for 3 min with distilled water. They were then immersed in Schiff's reagent (26052-06, Electron Microscopy Sciences) for 10 min. Next, the slides were washed for 5 min in distilled water. Nuclei were counterstained for 1 min with a hematoxylin solution following Mayer (3870, J.T. Baker, Center Valley, USA). The slides were then washed, dehydrated with xylene, and coverslipped with quick-mounting medium (Eukitt, Fluka Analytical, Germany).

### Immunofluorescence

Frozen sections were rehydrated with PBS and then blocked and permeabilized with 1% bovine serum albumin (Sigma-Aldrich) (Blocking buffer, BB) and 0.1% Triton X-100 (Sigma-Aldrich) in PBS for 20 min. They were washed with PBS and incubated with the corresponding primary antibodies overnight at 4°C. Slides were washed and incubated for 1 h at RT with the corresponding secondary antibodies. Nuclear staining was performed with Hoechst (H-33258, Fluka, Madrid, Spain), and slides were washed and coverslipped with Fluoromount (Electron Microscopy Sciences, Hatfield, PA, USA).

PF-paraffin-embedded sections were deparaffinized and required an antigen retrieval step before immunostaining. Thus, slides were immersed in sodium citrate buffer (10 mM, pH=6.0) heated to 100°C for 40 min and then cooled to RT for 30 min. The slides were washed, and the permeabilization step and immunofluorescence were then performed as described for the frozen sections.

The following were used as primary antibodies: rabbit monoclonal against GS (#15B1, Cell Signaling, Leiden, Netherlands); mouse monoclonal IgG1 against NeuN (#MAB377, MerckMillipore, Darmstadt, Germany); chicken polyclonal against GFAP (#AB5541, MerckMillipore); mouse monoclonal IgG2a against p62 (#ab56416, Abcam, Cambridge,

Author Manuscript Author Manuscript Author Manuscript Author Manuscript

UK); and human IgM purified immunoglobulins (OBT1524; AbD Serotec, Kidlington, UK). The following were used as secondary antibodies: Alexa Fluor (AF) 488 donkey anti-rabbit IgG (H+L); AF555 donkey anti-rabbit IgG (H+L); AF488 goat anti-chicken IgG (H+L); AF594 goat anti-mouse IgG1; AF594 goat anti-mouse IgG2a; and AF488 goat anti-human IgM heavy chain (Life Technologies, Eugene, OR, USA).

Staining controls were performed by incubating brain sections with BB instead of the primary antibody. In double staining, antibody cross-reactivity controls were also performed. In the case of p62 and GS staining, and in order to discard possible false positive staining produced by the presence of contaminant IgMs in the vials, secondary incubations with AF488 goat anti-mouse IgM (Jackson ImmunoResearch Laboratories) or goat anti-rabbit IgM conjugated to fluorescein isothiocyanate (FITC) (Abcam) antibodies were performed.

### Image acquisition

Images were taken with a fluorescence laser and optic microscope (BX41, Olympus, Germany) and stored in tiff format. In immunofluorescence studies, and for each staining, all images were acquired using the same microscope, laser and software settings. Image treatment and analysis were performed by means of the ImageJ program (National Institute of Health, USA).

### Quantification of the density of the different types of PGBs in mouse brain

To quantify the density of the different types of PGB (i.e. neuronal LBs (nLBs) and CAL granules) in the brains of mice from different strains, a minimum of four animals from each strain were used. Images of coronal sections were obtained with a Hamamatsu NanoZoomer Digital Slide Scanner (40× magnification). From each scanned coronal section, we then exported two tiff images containing the left and right brain hemispheres, each image including the hippocampus and the cortex from the retrosplenial granular region to the primary somatosensory cortex. The tiff images were then processed to calculate the number of nLBs or CAL granules using the ImageJ program (National Institute of Health, USA). For each tiff image, the process performed by this program included the following: a) splitting the color channels in order to obtain the green channel; b) transforming this new image into an 8-bit image; c) establishing the threshold in order to binarize the image; d) binarizing the image; d) applying the watershed; e) selecting, in the original image, the region where granules will be counted, i.e. the Region of Interest (ROI); f) saving the ROI in the ROI manager; g) applying the saved ROI in the corresponding binarized image; and h) to count the particles (i.e. PGBs) contained in the ROI. An example of image treatment and quantification of granules is summarized in Figure S1 (Supplementary material). To perform the quantification in non-continuous regions, we used the “combine” option in the ROI manager. The green channel of the original image was selected because it allowed better differentiation of the PGBs from other structures, such as nuclei and vessels walls. The threshold was visually and accurately set on each image, obtaining the best discrimination of granules. Watershed was applied because it allowed us to split some granules that were fused on binarized images. The size of particles to be counted was limited, in order to discard large structures. After the entire process, for each tiff image, we obtained the number of CAL granules in the hippocampus and in the cortex and that of nLBs in each of these regions in

Author Manuscript Author Manuscript Author Manuscript Author Manuscript

the case of malin$^{KO}$ mice (nLBs are present only in malin$^{KO}$ mice, not in the other strains studied). Finally, to obtain an approximation of the density of CAL or nLBs in a given hippocampal or cortical region, the total number of granules was divided by the total volume (area of the hippocampal or cortical region × section thickness). Data were tabulated for further descriptive and statistical analysis.

### Measurement of PGB size

To determine the size of the different types of PGB (i.e. nLBs and CAL granules) in malin$^{KO}$ animals, representative images from the brain cortex stained with the PAS method were acquired at a 40x magnification with a BX41 Olympus microscope (Germany). Four animals were used, and four images were acquired for each animal. The diameter of the PGBs in the images was then manually measured using the “straight” tool of the ImageJ program (National Institute of Health, USA). Data were tabulated for further descriptive and statistical analysis.

### Statistical analysis

Statistical analysis was performed with the ANOVA module of the IBM SPSS Statistics (IBM corp.©). Scheffe test was used for post-hoc comparisons. Significant differences were considered when $p<0.05$.

## Results

### Malin$^{KO}$ mice accumulate two types of PGB

To characterize and differentiate PGBs in mouse brain, several immunostainings were performed in control, malin$^{KO}$ and SAMP8 brain sections from animals aged 60–80 weeks. To detect PGBs, an antibody directed against GS, the only enzyme able to synthesize glucose polymers in mammals and a marker of PGBs (Vallés-Ortega *et al.* 2011), was used. Simultaneous fluorescence immunostaining on hippocampal sections with anti-GS and anti-GFAP antibodies allowed observation of the PGBs (Figure 1). As expected from previous descriptions (del Valle et al., 2010; Manich et al., 2016), a high number of astrocytic CAL granules were observed in SAMP8 mice (Figure 1a). These bodies were abundant in the hippocampus and tended to form clusters. The granules were in contact with astrocytic processes, as shown by GFAP staining, and, occasionally, the whole astrocyte that formed the cluster of granules was clearly visible. As previously indicated, CAL granules carry some neo-epitopes that are recognized by natural IgM antibodies, and the presence of these IgMs as contaminants in commercial antibodies has led to false positive staining and misinterpretations (Manich et al., 2015). In the present work, in order to discard false positive staining produced by such contaminant IgMs in the vial of anti-GS obtained in rabbit, we stained some sections with anti-GS as a primary antibody and a fluorochrome-labeled anti-rabbit IgM as a secondary antibody. The absence of staining on astrocytic CAL granules indicated that the anti-GS vial did not contain IgMs (Supplementary material, Figure S2), and thus confirmed that the GS staining of CAL granules was specific and not caused by IgMs. Of note, malin$^{KO}$ brain sections double immunostained with anti-GS and anti-GFAP also contained clusters of astrocytic CAL granules, which were distributed in practically all hippocampal layers (Figure 1b), while these clusters were observed only

Author Manuscript Author Manuscript Author Manuscript Author Manuscript

sporadically in the hippocampus of control animals (Figure 1c). In addition, the hippocampus of malin$^{KO}$ mice showed some PGBs that differed from CAL granules. These PGBs were located in the hippocampal pyramidal layer mainly of the CA2-CA3 region and were adjacent to nuclei, presumably neuronal nuclei (Figure 1b). These PGBs were spherical and appeared to be larger than astrocytic CAL granules, they did not form clusters, and they were unrelated to GFAP processes. SAMP8 and control animals did not present this second type of PGB. The PGBs that differed from astrocytic CAL granules were also detected in the brain cortex of malin$^{KO}$ mice (Figure 1e) but not in the cortex of control or SAMP8 animals (Figures 1d and f). In contrast, sporadic clusters of astrocytic CAL granules were detected in the cortex of the malin$^{KO}$ animals (Figure 1e). Thereafter, simultaneous immunostaining was also performed with anti-GS to label the PGBs and with NeuN antibody, which labels the perikarya of neuronal cells. These immunostainings confirmed that the hippocampal and cortical PGBs in malin$^{KO}$ mice that differ from astrocytic CAL granules are located inside the neuronal soma, near to the neuronal nuclei (Figure 2b and 2e). As these granules are exclusive to the malin$^{KO}$ mice (the model of LD) and are formed in neurons, we will refer to them as neuronal Lafora bodies (nLBs). CAL granules, visible in the SAMP8, malin$^{KO}$ and control animals with the anti-GS staining, did not colocalize with the neuronal NeuN staining.

To compare the size of astrocytic CAL granules with that of nLBs in malin$^{KO}$ mice, the size of the granules from the cortical region was measured on representative images from sections stained with PAS and obtained from four malin$^{KO}$ animals. A total of 259 CAL granules and 167 nLBs were measured. Thereafter, ANOVA was performed considering “size of granules” as the dependent variable, “type of granule” (nLB or CAL granule) as independent variable defined as a fixed factor and “animal” as independent variable defined as random factor. ANOVA indicated that the variable “type of granule” had a significant effect on “size of granules”, while the variable “animal” and the interaction between the independent variables did not. The mean size (±SEM) of CAL granules was 1.59 (±0.03) μm, while that of nLBs was 2.82 (±0.08) μm (Figures 3a and 3b). These observations allow us to conclude that nLBS attain larger sizes than CAL granules.

In the case of malin$^{KO}$ mice, we also determined the density of CAL granules and nLBs in the hippocampus and cortex of four animals. Thereafter, ANOVA was performed considering “density of granules” as the dependent variable and “type of granules” (CAL or nLBs), “brain region” (hippocampus or cortex) and “animal” as independent variables. The variables “type of granules” and “brain region” were defined as fixed factors and “animal” as random factor. The ANOVA indicated that the variables “type of granules” and “brain region” and the interaction between them had a significant effect on “density of granules”. The mean density (±SEM) of the CAL granules in the cortex and hippocampus was 4936.45 (±594.91) granules/mm$^3$ and 176709.32 (±16058.40) granules/mm$^3$ respectively, and the mean density (±SEM) of nLBs in the cortex and hippocampus was 33671.06 (±2217.18) granules/mm$^3$ and 9324.92 (±592.69) granules/mm$^3$, respectively (Figure 3d). Post hoc comparisons indicated that the density of CAL granules was higher in the hippocampus than in the cortex, the density of nLBs was higher in the cortex than in the hippocampus, the density of CAL granules in the hippocampus was higher than that of nLBs in the hippocampus, and the density of nLBs in the cortex was higher than the density of CAL

Author Manuscript Author Manuscript Author Manuscript Author Manuscript

granules in the cortex. These results indicate that CAL granules predominate in the hippocampus while nLBs predominate in the cortex. Of note is the high density of CAL granules in the hippocampus compared to the other densities measured.

As CAL granules are also present in SAMP8 and control animals, we also determined the density of astrocytic CAL granules in each brain region in these mouse strains. In this case, ANOVA was performed considering “density of granules” as the dependent variable and “strain” (SAMP8, malin$^{KO}$ and control) and “brain region” (hippocampus or cortex) as the independent variables, defined as fixed factors. ANOVA indicated that the variables “strain” and “brain region” had a significant effect on “density of granules” and the interaction between both variables is also significant. In SAMP8 animals, the mean density (±SEM) of the CAL granules in the hippocampus was 27560.24 (±1742.26) granules/mm$^3$. In malin$^{KO}$ animals, as indicated before, the mean density (±SEM) of CAL granules in the cortex and hippocampus was 4936.45 (±594.91) granules/mm$^3$ and 176709.32 (±16058.40) granules/mm$^3$, respectively. In control animals, the mean density (±SEM) of CAL granules in the hippocampus was 2388.17 (±428.63) granules/mm$^3$. CAL granules were not observed in the cortex of SAMP8 or control animals. Histograms of mean densities are shown in Figure 3e. The results indicate that the density of CAL granules was higher in the hippocampus than in the cortex in all the mouse strains and that the density of CAL granules was higher in malin$^{KO}$ and SAMP8 animals than in controls, being also higher in malin$^{KO}$ than in SAMP8 mice. Thus, we can assume that the absence of malin in malin$^{KO}$ animals enhances the formation of CAL granules, although this increase can also be observed in other conditions like senescence, as observed in SAMP8 animals.

Taken together, these observations indicate that malin$^{KO}$ animals present two types of PGB: a) CAL granules, which tend to form clusters, are associated with astrocytes, and predominate in the hippocampus, although some clusters can also be observed in the cortex; and b) nLBs, which are larger than CAL granules, are isolated granules, are related to neurons, and are found in the brain cortex and the pyramidal layer of the hippocampus. Of note, nLBs were exclusive to malin$^{KO}$ mice, while astrocytic CAL granules, which were also present in SAMP8 and in control animals, were enhanced in both malin$^{KO}$ and SAMP8 animals. These results are summarized in Table I.

## Astrocytic CAL granules, but not nLBs, carry neo-epitopes recognized by natural IgMs

Human CA, as well as CAL granules of SAMP8 and ICR-CD1 mice, contain neo-epitopes that can be recognized by natural IgMs (Augé et al., 2017; Manich et al., 2015). To analyze whether PGBs from malin$^{KO}$ mice also carry these neo-epitopes, double immunostaining was performed with anti-GS and purified human IgMs in the first incubation and the fluorochrome-labeled respective isotype specific antibodies in the second one. As expected, astrocytic CAL granules were immunostained with both antibodies, thereby revealing the presence of neo-epitopes on these structures (Figure 4a). In contrast, nLBs were not positive for IgMs, thus indicating the absence of neo-epitopes (Figure 4b). All together, these observations reveal that the two types of PGB found in malin$^{KO}$ animals differ in terms of neo-epitope presence.

Author Manuscript Author Manuscript Author Manuscript Author Manuscript

### Polyglucosan structure of CAL granules is required for the presence of the neo-epitopes

The brains of MGS$^{KO}$ mice do not present PGBs and, consequently, MGS activity is a requisite for the formation of these bodies (Sinadinos et al., 2014; Duran et al., 2014). Accordingly, we examined whether the absence of the astrocytic CAL granules in MGS$^{KO}$ animals (76–80 weeks-old) correlated with the absence of the neo-epitopes. Accordingly, we immunostained brain sections from MGS$^{KO}$ animals with both anti-GS antibody and human IgMs. As expected, CAL granules were not detected with the anti-GS antibody in any brain region. Moreover, staining with human IgMs did not reveal the presence of neo-epitopes either (Figure 5). These results suggest that the neo-epitopes are part of the polyglucosan structure of the PGBs or that this polyglucosan structure is required for the addition of components that carry the neo-epitopes.

### PTG$^{OE}$ mice present CAL granules but not nLBs

PTG is a protein that orchestrates the signaling of several metabolic enzymes involved in glycogen synthesis. In this regard, the brains of PTG$^{OE}$ mice show enhanced PGB accumulation (Duran et al., 2014). We therefore examined the nature of these PGBs and the presence of neo-epitopes on them. Double immunostaining with both the anti-GS antibody and human IgMs in brain sections of PTG$^{OE}$ mice aged 60–64 weeks showed the presence of CAL granules, forming the characteristic clusters. These granules were immunostained with both anti-GS antibody and human IgMs and were located mainly in the hippocampus (Figure 6). No nLBs were found in this mouse model. Based on these observations, we postulate that the overexpression of PTG is not sufficient to trigger the formation of nLBs in neurons but is sufficient to increase the formation of CAL granules in astrocytes.

### p62 is present in both CAL granules and nLBs

p62 is an ubiquitin-binding scaffold protein that interacts with ubiquitinated proteins via its C-terminal ubiquitin-associated (UBA) domain. The direct binding of p62 to LC3 and GABARAP family proteins, that serves as membrane linked protein-binding platforms (Qiu et al., 2017), allows p62 to guide ubiquitinated proteins to autophagosomes and to autophagic processes (Isakson et al., 2013). Moreover, p62 is also related to secretory autophagy, in which the content of the autophagosome is extruded from the cell (Ponpuak et al., 2016). Impaired autophagy has been described in LD mouse models, and it has been reported that p62 is increased in the brains of malin$^{KO}$ mice (Duran et al., 2014). To determine whether the PGBs of malin$^{KO}$ mice contain this protein, we performed double immunostaining with anti-GS and anti-p62 antibodies on brain sections of these animals. Both CAL granules and nLBs were stained with anti-p62 antibody, thereby indicating the presence of these proteins in both types of PGB (Figure 7). The presence of p62 in nLBs, which are located in the neuronal soma, near the nuclei, suggests that nLBs are related to lysosomal degradative autophagy. CAL granules, however, are located in astrocytic processes. As we will further discuss, the presence of p62 in these cells is perhaps related to secretory autophagy. It should be noted that to avoid false staining produced by contaminant IgMs in the vial, in the second incubations we used specific anti-IgG secondary antibodies that do not recognize the IgMs. In a complementary manner, and as performed for the anti-GS, we also examined whether mouse IgMs were present in the vial of anti-p62 antibody

Author Manuscript Author Manuscript Author Manuscript Author Manuscript

obtained in mouse. To this end, we stained some sections with anti-p62 antibody in the first incubation and with a secondary fluorochrome-labeled anti-mouse IgM antibody in the second one. The absence of staining in CAL granules indicated that the anti-p62 vial did not contain IgMs (Supporting Information, Figure S2).

## Discussion

LD is characterized by the accumulation of PBGs in the brain, in the form of the so-called LBs. Traditionally, LBs are considered to be neuronal inclusions that occur concomitantly with neurodegeneration and epilepsy and they are related to the inexorable worsening of the condition until death in early adulthood (Lafora & Glueck, 1911). The extensive neuronal loss and severe neuropathological phenotypes observed in patients and animal models of LD suggest that neurons are particularly vulnerable to excess glycogen accumulation (Delgado-Escueta, 2007; Duran et al., 2014; López-González et al., 2017; Vallés-Ortega et al., 2011). Consistent with this, we have demonstrated that glycogen accumulation in neurons induces their death by apoptosis (Duran et al., 2012).

In this study, however, we demonstrate that malin$^{KO}$ mice present high numbers of two types of PGB in the brain, one affecting neurons (nLBs) and the other astrocytes (CAL granules). The CAL granules, referred to in some cases as “PAS granules” in the literature, are also abundant in SAMP8 mice and in aged mice of other strains (Akiyama et al., 1986; Jucker et al., 1994b; Kuo et al., 1996; Manich et al., 2011; Manich et al., 2014a). We observed that the number of CAL granules was also increased in PTG$^{OE}$ mice, indicating that the enhanced activity of MGS promotes their formation. Also, we found that CAL granules were absent in MGS$^{KO}$ animals, thereby indicating that the synthesis of glycogen is indispensable for their formation. In a recent study, Oe et al. (2016) found that levels of glycogen from young C57BL/6 mice were high in the hippocampus. The accumulation of this glycogen was mainly in astrocytes, predominantly in their processes. In addition, these cells showed a patchy distribution of glycogen, each patch corresponding to an individual astrocyte. This patchy distribution diminished in aged mice, when PGBs appeared. The results obtained in the study by Oe et al. are thus consistent with our work, considering that the shifting from patchy glycogen to aberrant polyglucosan that forms the PGBs could be enhanced in malin$^{KO}$, PTG$^{OE}$ and SAMP8 but not in MGS$^{KO}$ animals. The other type of PGB that we found in malin$^{KO}$ mice, located in the perikarya of the neurons, near to neuronal nuclei, and referred to here as nLBs, appears to be exclusive to this animal model since it has not been observed in any other strain. All together, these results indicate that the absence of malin triggers the formation of PGBs in neurons and enhances the development of these bodies in astrocytes.

Accordingly, although it is widely assumed that all the PGBs in the brains of LD patients are neuronal, we propose that the two types of PGB described here are present: one type, probably CA, derived from astrocytes and the other type derived from neurons. Therefore, the term LBs should be limited to refer to nLBs. Moreover, based on the observations made in the malin$^{KO}$ mouse model, the amount of the different types of PGB in the brains of LD patients is expected to be dependent on the brain region. The probable significant presence of both types of PGB in the brains of these individuals reinforces the need to make a

Author Manuscript Author Manuscript Author Manuscript Author Manuscript

distinction between LBs and CA, as previously stressed by various authors (Cervós-Navarro, 1991; Leel-Ossy, 2001; Ramsey, 1964; Seitelberger, 1968; Yoshimura, 1977).

As indicated earlier, we previously described the presence of neo-epitopes on both CAL granules from mouse brains and CA from human brains (Augé et al., 2017; Manich et al., 2014b). Although the composition of CA must be re-examined due to the possible false positive staining in immunohistochemical studies (Augé et al., 2017), there is wide consensus that CA contain waste products (Cavanagh, 1999; Pirici and Margaritescu, 2014) and ubiquitin (Cissé et al., 1995; Day et al., 2015; Pirici et al., 2014; Pirici and Margaritescu, 2014; Wilhelmus et al., 2011). It has been proposed that the presence of neo-epitopes on CA is related to the removal of these bodies via the natural immune system after their extrusion (Augé et al., 2017). In this regard, here we show that CAL granules contain p62 protein, which has a ubiquitin-binding domain and is involved in the sequestration of ubiquitinated proteins and organelles (Liu et al., 2016). Also, p62 is related to secretory autophagy, a process in which the content of the autophagosome extrudes from the cell (Ponpuak et al., 2016). Therefore, the presence of p62 in CAL granules is consistent with the extrusion of CA from human brains.

Furthermore, the presence of a high number of CAL granules in the malin$^{KO}$ mouse model suggests that the absence of malin alters glycogen metabolism not only in neurons but also in astrocytes. In the case of PTG$^{OE}$ mice, CAL granules, but not nLBs, are also present in high numbers. This observation thus indicates distinct routes or key regulators in the genesis of nLBs and CAL granules. However, the activity of MGS is required for the formation of both types of granule, as can be deduced from the observation that CAL granules are absent in MGS$^{KO}$ animals and that both types of PGB are absent in the double mutant malin$^{KO}$ +MGS$^{KO}$ mouse (Duran et al., 2014). CAL granules differ from nLBs in terms of distribution in the brain, size, clustering, and presence of neo-epitopes recognized by IgMs. We previously described the presence of PGBs in astrocytes of the malin$^{KO}$ mouse model (Valles-Ortega et al., 2011). In the present work, we identify astrocytic PGBs as CAL granules and an important pool of PGBs in LD. Since astrocytes serve essential roles in brain function, the impairment of astrocytic activity caused by the accumulation of CAL granules may contribute to the pathophysiology of LD. In this regard, astrocytic uptake of potassium and glutamate is essential for the regulation of neuronal excitability, and the malfunction of astrocytes in LD could explain the epileptic phenotype of the disease (Amédée et al., 1997; Coulter and Eid, 2012). Given that aged mice and the PTG$^{OE}$ mouse model show increased accumulation of CAL granules, it would be of interest to study the epileptic phenotype of these animals.

LBs have been classified as type I or type II on the basis of their size and shape (Van Hoof et al., 1967; Machado-Salas J et al., 2012). Furthermore, it has been hypothesized that these two types are different stages of the same process, in which the accumulation of type I LBs would activate the formation of type II LBs (Machado-Salas et al., 2012). On the basis of the results and images presented in that study, it seems that type I LBs correspond to CAL granules and type II to nLBs. Therefore, if this correspondence is correct, it is not possible that type I LBs would activate the formation of type II, because of the different cellular origin and different brain region preferences of CAL granules and nLBs. Moreover, given

Author Manuscript Author Manuscript Author Manuscript Author Manuscript

the presence of possible IgM contaminants in the antibodies used and the false staining that IgMs can produce (Manich et al., 2015), we propose that immunohistochemistry studies of PGBs should be reanalyzed.

In conclusion, here we report that the absence of malin enhances the formation of astrocytic CAL granules and triggers the formation of nLBs. These findings should be considered when studying LD, and further work should be done to determine the involvement of each type of PGB in the etiopathogeny of this disease. Greater knowledge of the effects of CAL granules on astrocytes and those of nLBs on neurons, as well as the interaction between the neo-epitopes present in CAL granules and the natural immune system, is expected to contribute to unravelling LD.

## Supplementary Material

Refer to Web version on PubMed Central for supplementary material.

## Acknowledgments

IRB Barcelona is the recipient of a Severo Ochoa Award of Excellence from MINECO (Government of Spain). This study was supported by grants BFU2013-47382-P, SAF-2014-54525-P and BFU2016-78398-P from MINECO, by the Agencia Estatal de Investigación (AEI), by European Regional Development Funds and a grant from the National Institute of Health (NIH-NINDS) P01NS097197. It was also funded by *CIBER de Diabetes y Enfermedades Metabólicas* and *CIBER de Enfermedades Neurodegenerativas* from the *Instituto de Salud Carlos III*. We thank the *Generalitat de Catalunya* for funding our research group (2014/SGR525). I. Cabezón and E. Augé received pre-doctoral "Ajuts de Personal Investigador en Formació" fellowships from the *Universitat de Barcelona* (APIF-UB). None of the supporting agencies had any role in performing the study or writing the manuscript.

## References

Aguado C, Sarkar S, Korolchuk VI, Criado O, Vernia S, Boya P, Sanz P, de Córdoba SR, Knecht E, Rubinsztein DC. Laforin, the most common protein mutated in Lafora disease, regulates autophagy. Human Molecular Genetics. 2010; 19:2867–2876. DOI: 10.1093/hmg/ddq190 [PubMed: 20453062]

Akiyama H, Kameyama M, Akiguchi I, Sugiyama H, Kawamata T, Fukuyama H, Kimura H, Matsushita M, Takeda T. Periodic acid-Schiff (PAS)-positive: granular structures increase in the brain of senescence accelerated mouse (SAM). Acta Neuropathologica. 1986; 72:124–129. [PubMed: 3825511]

Amédée T, Robert A, Coles JA. Potassium homeostasis and glial energy metabolism. Glia. 1997; 21:46–55. [PubMed: 9298846]

Augé E, Cabezón I, Pelegrí C, Vilaplana J. New perspectives on corpora amylacea in the human brain. Scientific Reports. 2017; 7:41807.doi: 10.1038/srep41807 [PubMed: 28155917]

Baumgarth N, Tung JW, Herzenberg LA. Inherent specificities in natural antibodies: a key to immune defense against pathogen invasion. Springer Seminars in Immunopathology. 2005; 26:347–362. DOI: 10.1007/s00281-004-0182-2 [PubMed: 15633017]

Binder CJ. Natural IgM antibodies against oxidation-specific epitopes. Journal of Clinical Immunology. 2010; 30:S56–S60. DOI: 10.1007/s10875-010-9396-3 [PubMed: 20387104]

Cavanagh JB. Corpora-amylacea and the family of polyglucosan diseases. Brain Research Reviews. 1999; 29:265–295. [PubMed: 10209236]

Cervós-Navarro J. Pathologie des Nervensystems V: Degenerative und metabolische Erkrankungen. Berlin, Germany: Springer Verlag; 1991. Polyglukosaneinschlüsse im Nervengewebe.

Chan EM, Young EJ, Ianzano L, Munteanu I, Zhao X, Christopoulos CC, Avanzini G, Elia M, Ackerley CA, Jovic NJ, Bohlega S, Andermann E, Rouleau GA, Delgado-Escueta AV, Minassian BA, Scherer SW. Mutations in NHLRC1 cause progressive myoclonus epilepsy. Nature Genetics. 2003; 35:125–127. DOI: 10.1038/ng1238 [PubMed: 12958597]

Author Manuscript Author Manuscript Author Manuscript Author Manuscript

Cheng A, Zhang M, Gentry MS, Worby CA, Dixon JE, Saltiel AR. A role for AGL ubiquitination in the glycogen storage disorders of Lafora and Cori's disease. Genes & Development. 2007; 21:2399–2409. DOI: 10.1101/gad.1553207 [PubMed: 17908927]

Cissé S, Perry G, Lacoste-Royal G, Cabana T, Gauvreau D. Immunochemical identification of ubiquitin and heat-shock proteins in corpora amylacea from normal aged and Alzheimer's disease brains. Acta Neuropathologica. 1993; 85:233–240. [PubMed: 7681614]

Coulter DA, Eid T. Astrocytic regulation of glutamate homeostasis in epilepsy. Glia. 2012; 60:1215–1226. DOI: 10.1002/glia.22341 [PubMed: 22592998]

Criado O, Aguado C, Gayarre J, Duran-Trio L, Garcia-Cabrero AM, Vernia S, San Millán B, Heredia M, Romá-Mateo C, Mouron S, Juana-López L, Domínguez M, Navarro C, Serratosa JM, Sanchez M, Sanz P, Bovolenta P, Knecht E, Rodriguez de Cordoba S. Lafora bodies and neurological defects in malin-deficient mice correlate with impaired autophagy. Human Molecular Genetics. 2012; 21:1521–1533. DOI: 10.1093/hmg/ddr590 [PubMed: 22186026]

Day RJ, Mason MJ, Thomas C, Poon WW, Rohn TT. Caspase-cleaved tau co-localizes with early tangle markers in the human vascular dementia brain. PLOS One. 2015; 10:e0132637.doi: 10.1371/journal.pone.0132637 [PubMed: 26161867]

Del Valle J, Duran-Vilaregut J, Manich G, Casadesús G, Smith MA, Camins A, Pallàs M, Pelegrí C, Vilaplana J. Early amyloid accumulation in the hippocampus of SAMP8 mice. Journal of Alzheimer's disease. 2010; 19:1303–1315. DOI: 10.3233/JAD-2010-1321

Delgado-Escueta AV. Advances in Lafora progressive myoclonus epilepsy. Current Neurology and Neuroscience Reports. 2007; 7:428–433. [PubMed: 17764634]

Doehner J, Madhusudan A, Konietzko U, Fritschy JM, Knuesel I. Co-localization of Reelin and proteolytic AbetaPP fragments in hippocampal plaques in aged wild-type mice. Journal of Alzheimer's Disease. 2010; 19:1339–1357. DOI: 10.3233/JAD-2010-1333

Duran J, Guinovart JJ. Brain glycogen in health and disease. Molecular Aspects of Medicine. 2015; 46:70–77. DOI: 10.1016/j.mam.2015.08.007 [PubMed: 26344371]

Duran J, Tevy MF, Garcia-Rocha M, Calbó J, Milán M, Guinovart JJ. Deleterious effects of neuronal accumulation of glycogen in flies and mice. EMBO Molecular Medicine. 2012; 4:719–729. DOI: 10.1002/emmm.201200241 [PubMed: 22549942]

Duran J, Saez I, Gruart A, Guinovart JJ, Delgado-García JM. Impairment in long-term memory formation and learning-dependent synaptic plasticity in mice lacking glycogen synthase in the brain. Journal of Cerebral Blood Flow and Metabolism. 2013; 33:550–556. DOI: 10.1038/jcbfm.2012.200 [PubMed: 23281428]

Duran J, Gruart A, Garcia-Rocha M, Delgado-Garcia JM, Guinovart JJ. Glycogen accumulation underlies neurodegeneration and autophagy impairment in Lafora disease. Human Molecular Genetics. 2014; 23:3147–3156. DOI: 10.1093/hmg/ddu024 [PubMed: 24452334]

Garyali P, Siwach P, Singh PK, Puri R, Mittal S, Sengupta S, Parihar R, Ganesh S. The malin-laforin complex suppresses the cellular toxicity of misfolded proteins by promoting their degradation through the ubiquitin-proteasome system. Human Molecular Genetics. 2009; 18:688–700. DOI: 10.1093/hmg/ddn398 [PubMed: 19036738]

Gayarre J, Duran-Trio L, Garcia OC, Aguado C, Juana-Lopez L, Crespo I, Knecht E, Bovolenta P, de Cordoba SR. The phosphatase activity of laforin is dispensable to rescue Epm2a−/− mice from Lafora disease. Brain. 2014; 137:806–818. DOI: 10.1093/brain/awt353 [PubMed: 24430976]

Grönwall C, Vas J, Silverman GJ. Protective roles of natural IgM antibodies. Frontiers in Immunology. 2012; 3:66.doi: 10.3389/fimmu.2012.00066 [PubMed: 22566947]

Hamamoto H, Honma A, Irino M, Matsushita T, Toda K, Matsumura M, Takeda T. Grading score system: A method for evaluation of the degree of senescence in senescence accelerated mouse (SAM). Mechanisms of Ageing and Development. 1984; 26:91–102. [PubMed: 6748759]

Isakson P, Holland P, Simonsen A. The role of ALFY in selective autophagy. Cell Death and Differentiation. 2103; 20:12–20.

Jucker M, Walker LC, Kuo H, Tian M, Ingram DK. Age-related fibrillar deposits in brains of C57BL/6 mice. A review of localization, staining characteristics, and strain specificity. Molecular Neurobiology. 1994a; 9:125–133. [PubMed: 7534088]

Author Manuscript Author Manuscript Author Manuscript Author Manuscript

Jucker M, Walker LC, Schwarb P, Hengemihle J, Kuo H, Snow AD, Bamert F, Ingram DK. Age-related deposition of glia-associated fibrillar material in brains of C57BL/6 mice. Neuroscience. 1994b; 60:875–889. [PubMed: 7936209]

Knecht E, Aguado C, Sarkar S, Korolchuk VI, Criado-Garcia O, Vernia S, Boya P, Sanz P, Rodríguez de Córdoba S, Rubinsztein DC. Impaired autophagy in Lafora disease. Autophagy. 2010; 6:991–993. DOI: 10.4161/auto6.7.13308 [PubMed: 20818165]

Kuo H, Ingram DK, Walker LC, Tian M, Hengemihle JM, Jucker M. Similarities in the age-related hippocampal deposition of periodic acid-schiff-positive granules in the senescence-accelerated mouse P8 and C57BL/6 mouse strains. Neuroscience. 1996; 74:733–740. [PubMed: 8884769]

Lafora GR, Glueck B. Beitrag zur Histopathologie der myoklonischen epilepsie. Zeitschrift für die Gesamte Neurologie und Psychiatrie. 1911; 6:1–14.

Leel-Ossy L. New data on the ultrastructure of the corpus amylaceum (polyglucosan body). Pathology Oncology Research. 2001; 7:145–150. [PubMed: 11458279]

López-González I, Viana R, Sanz P, Ferrer I. Inflammation in Lafora disease: Evolution with disease progression in laforin and malin knock-out mouse models. Molecular Neurobiology. 2017; 54:3119–3130. DOI: 10.1007/s12035-016-9884-4 [PubMed: 27041370]

Liu WJ, Ye L, Huang WF, Gui LJ, Xu G, Wu HL, Yang C, Liu HF. p62 links the autophagy pathway and the ubiquitin-proteosome system upon ubiquitinated protein degradation. Cellular & Molecular Biology Letters. 2016; 13:21–29. DOI: 10.1186/s11658-016-0031-z

Machado-Salas J, Avila-Costa MR, Guevara P, Guevara J, Durón RM, Bai D, Tanaka M, Yamakawa K, Delgado-Escueta AV. Ontogeny of Lafora bodies and neurocytoskeleton changes in Laforin-deficient mice. Experimental Neurology. 2012; 236:131–140. DOI: 10.1016/j.expneurol.2012.04.008 [PubMed: 22542948]

Madhusudan A, Sidler C, Knuesel I. Accumulation of reelin-positive plaques is accompanied by a decline in basal forebrain projection neurons during normal aging. The European Journal of Neuroscience. 2009; 30:1064–1076. DOI: 10.1111/j.1460-9568.2009.06884.x [PubMed: 19735296]

Manich G, Augé E, Cabezón I, Pallàs M, Vilaplana J, Pelegrí C. Neo-epitopes emerging in the neurodegenerative hippocampal granules of aged mice can be recognized by natural IgM auto-antibodies. Immunity & Ageing. 2015; 12:23.doi: 10.1186/s12979-015-0050-z [PubMed: 26604974]

Manich G, Cabezón I, Augé E, Pelegrí C, Vilaplana J. Periodic acid-Schiff granules in the brain of aged mice: From amyloid aggregates to degenerative structures containing neo-epitopes. Ageing Research Reviews. 2016; 27:42–55. DOI: 10.1016/j.arr.2016.03.001 [PubMed: 26970374]

Manich G, Cabezón I, Camins A, Pallàs M, Liberski PP, Vilaplana J, Pelegrí C. Clustered granules present in the hippocampus of aged mice result from a degenerative process affecting astrocytes and their surrounding neuropil. Age. 2014a; 36:9690.doi: 10.1007/s11357-014-9690-8 [PubMed: 25070375]

Manich G, Del Valle J, Cabezón I, Camins A, Pallàs M, Pelegrí C, Vilaplana J. Presence of a neo-epitope and absence of amyloid beta and tau protein in degenerative hippocampal granules of aged mice. Age. 2014b; 36:151–165. DOI: 10.1007/s11357-013-9560-9 [PubMed: 23867972]

Minassian BA. Lafora's disease: towards a clinical, pathologic, and molecular synthesis. Pediatric Neurology. 2001; 25:21–29. [PubMed: 11483392]

Minassian BA, Lee JR, Herbrick JA, Huizenga J, Soder S, Mungall AJ, Dunham I, Gardner R, Fong CY, Carpenter S, Jardim L, Satishchandra P, Andermann E, Snead OC, Lopes-Cendes I, Tsui LC, Delgado-Escueta AV, Rouleau GA, Scherer SW. Mutations in a gene encoding a novel protein tyrosine phosphatase cause progressive myoclonus epilepsy. Nature Genetics. 1998; 20:171–174. [PubMed: 9771710]

Nitschke F, Sullivan MA, Wang P, Zhao X, Chown EE, Perri AM, Israelian L, Juana-Lopez L, Bovolenta P, Rodriguez de Cordoba S, Steup M, Minassian BA. Abnormal glycogen chain length pattern, not hyperphosphorylation, is critical in Lafora disease. EMBO Molecular Medicine. 2017; 9:906–917. DOI: 10.15252/emmm.201707608 [PubMed: 28536304]

Author Manuscript Author Manuscript Author Manuscript Author Manuscript

Oe Y, Baba O, Ashida H, Nakamura KC, Hirase H. Glycogen distribution in the microwave-fixed mouse brain reveals heterogeneous astrocytic patterns. Glia. 2016; 64:1532–1545. DOI: 10.1002/glia.23020 [PubMed: 27353480]

Pirici I, Margaritescu C, Mogoanta L, Petrescu F, Simionescu CE, Popescu ES, Cecoltan S, Pirici D. Corpora amylacea in the brain form highly branched three-dimensional lattices. Romanian Journal of Morphology and Embryology. 2014; 55:1071–1077. [PubMed: 25607387]

Pirici D, Margaritescu C. Corpora amylacea in aging brain and age-related brain disorders. Journal of Aging Gerontology. 2014; 2:33–57. http://dx.doi.org/10.12974/2309-6128.2014.02.01.6.

Puri R, Suzuki T, Yamakawa K, Ganesh S. Dysfunctions in endosomal-lysosomal and autophagy pathways underlie neuropathology in a mouse model for Lafora disease. Human Molecular Genetics. 2012; 21:175–184. DOI: 10.1093/hmg/ddr452 [PubMed: 21965301]

Qiu Y, Zheng Y, Wu KP, Schulman BA. Insights into links between autophagy and the ubiquitin system from the structure of LC3B bound to the LIR motif from the E3 ligase NEDD4. Protein Science. 2017; 26:1674–1680. DOI: 10.1002/pro.3186 [PubMed: 28470758]

Ramsey HI. Ultrastructure of corpora amylacea. Journal of Neuropathology and Experimental Neurology. 1965; 24:25–39. [PubMed: 14253571]

Rao SN, Maity R, Sharma J, Dey P, Shankar SK, Satishchandra P, Jana NR. Sequestration of chaperones and proteasome into Lafora bodies and proteasomal dysfunction induced by Lafora disease-associated mutations of malin. Human Molecular Genetics. 2010; 19:4726–4734. DOI: 10.1093/hmg/ddq407 [PubMed: 20858601]

Roach PJ. Glycogen phosphorylation and Lafora disease. Molecular Aspects of Medicine. 2015; 46:78–84. DOI: 10.1016/j.mam.2015.08.003 [PubMed: 26278984]

Robertson TA, Dutton NS, Martins RN, Roses AD, Kakulas BA, Papadimitriou JM. Age-related congophilic inclusions in the brains of apolipoprotein E-deficient mice. Neuroscience. 1998; 82:171–180. [PubMed: 9483513]

Rohn TT. Corpora amylacea in neurodegenerative diseases: cause or effect? International Journal of Neurology and Neurotherapy. 2015; 2:3.

Sbarbati A, Carner M, Colletti V, Osculati F. Extrusion of corpora amylacea from the marginal glia at the vestibular root entry zone. Journal of Neuropathology Experimental Neurology. 1996; 55:196–201. [PubMed: 8786378]

Seitelberger F. Pathology of the nervous system. New York, NY: NMcGraw-Hill; 1968. Myoclonus body disease.

Serratosa JM, Gomez-Garre P, Gallardo ME, Anta B, de Bernabe DB, Lindhout D, Augustijn PB, Tassinari CA, Malafosse RM, Topcu M, Grid D, Dravet C, Berkovic SF, De Córdoba SR. A novel protein tyrosine phosphatase gene is mutated in progressive myoclonus epilepsy of the Lafora type (*EPM2*). Human Molecular Genetics. 1999; 8:345–352. [PubMed: 9931343]

Sharma J, Rao SN, Shankar SK, Satishchandra P, Jana NR. Lafora disease ubiquitin ligase malin promotes proteasomal degradation of neuronatin and regulates glycogen synthesis. Neurobiology of Disease. 2011; 44:133–141. DOI: 10.1016/j.nbd.2011.06.013 [PubMed: 21742036]

Sinadinos C, Valles-Ortega J, Boulan L, Solsona E, Tevy MF, Marquez M, Duran J, Lopez-Iglesias C, Calbó J, Blasco E, Pumarola M, Milán M, Guinovart JJ. Neuronal glycogen synthesis contributes to physiological aging. Aging Cell. 2014; 13:935–945. DOI: 10.1111/acel.12254 [PubMed: 25059425]

Suzuki A, Yokoo H, Kakita A, Takahashi H, Harigaya Y, Ikota H, Nakazato Y. Phagocytized corpora amylacea as a histological hallmark of astrocytic injury in neuromyelitis optica. Neuropathology. 2012; 32:597–594. DOI: 10.1111/j.1440-1789.2012.01299.x

Tagliabracci VS, Girard JM, Segvich D, Meyer C, Turnbull J, Zhao XC, Minassian BA, DePaoli-Roach AA, Roach PJ. Abnormal metabolism of glycogen phosphate as a cause for Lafora disease. Journal of Biological Chemistry. 2008; 283:33816–33825. DOI: 10.1074/jbc.M807428200 [PubMed: 18852261]

Tagliabracci VS, Turnbull J, Wang W, Girard JM, Zhao X, Skurat AV, Delgado-Escueta AV, Minassian BA, DePaoli-Roach AA, Roach PJ. Laforin is a glycogen phosphatase, deficiency of which leads to elevated phosphorylation of glycogen in vivo. Proceedings of the National Academy of Sciences USA. 2007; 104:19262–19266. DOI: 10.1073/pnas.0707952104

Author Manuscript Author Manuscript Author Manuscript Author Manuscript

Takeda T, Hosokawa M, Higuchi K. Senescence accelerated mouse (SAM), a novel murine model of aging. The SAM model of senescence. Takeda T, editorElsevier; Amsterdam: 1994. 15–22.

Valles-Ortega J, Duran J, Garcia-Rocha M, Bosch C, Saez I, Pujadas L, Serafin A, Cañas X, Soriano E, Delgado-García JM, Gruart A, Guinovart JJ. Neurodegeneration and functional impairments associated with glycogen synthase accumulation in a mouse model of Lafora disease. EMBO Molecular Medicine. 2011; 3:667–681. DOI: 10.1002/emmm.201100174 [PubMed: 21882344]

Van Hoof F, Hageman-Bal M. Progressive familial myoclonic epilepsy with Lafora bodies. Electron microscopic and histochemical study of a cerebral biopsy. Acta Neuropathologica. 1967; 7:315–336. [PubMed: 4166286]

Vilchez D, Ros S, Cifuentes D, Pujadas L, Valles J, Garcia-Fojeda B, Criado-García O, Fernández-Sánchez E, Medraño-Fernández I, Domínguez J, García-Rocha M, Soriano E, Rodríguez de Córdoba S, Guinovart JJ. Mechanism suppressing glycogen synthesis in neurons and its demise in progressive myoclonus epilepsy. Nature Neuroscience. 2007; 10:1407–1413. DOI: 10.1038/nn1998 [PubMed: 17952067]

Wilhelmus MMM, Verhaar R, Bol JG, Van Dam AM, Hoozemans JJ, Rozemuller AJ, Drukarch B. Novel role of transglutaminase 1 in corpora amylacea formation? Neurobiology of Aging. 2011; 32:845–856. DOI: 10.1016/j.neurobiolaging.2009.04.019 [PubMed: 19464759]

Worby CA, Gentry MS, Dixon JE. Malin decreases glycogen accumulation by promoting the degradation of protein targeting to glycogen (PTG). The Journal of Biological Chemistry. 2008; 283:4069–4076. DOI: 10.1074/jbc.M708712200 [PubMed: 18070875]

Yoshimura T. Beiträge zu den klinisch - und histopathologischen Untersuchungen über die Fälle der Lafora-ähnlichen Einschlusskörperchen. Folia Psychiatrica et Neurologica Japonica. 1977; 31:89–102. [PubMed: 193769]

Author Manuscript Author Manuscript Author Manuscript Author Manuscript

**Main points**

- Absence of malin triggers the formation of polyglucosan bodies in neurons and enhances their development in astrocytes.
- These astrocytic polyglucosan bodies contain neo-epitopes that are recognized by natural antibodies.
- Astrocytes are involved in the etiopathogenesis of Lafora disease.

Author Manuscript Author Manuscript Author Manuscript Author Manuscript

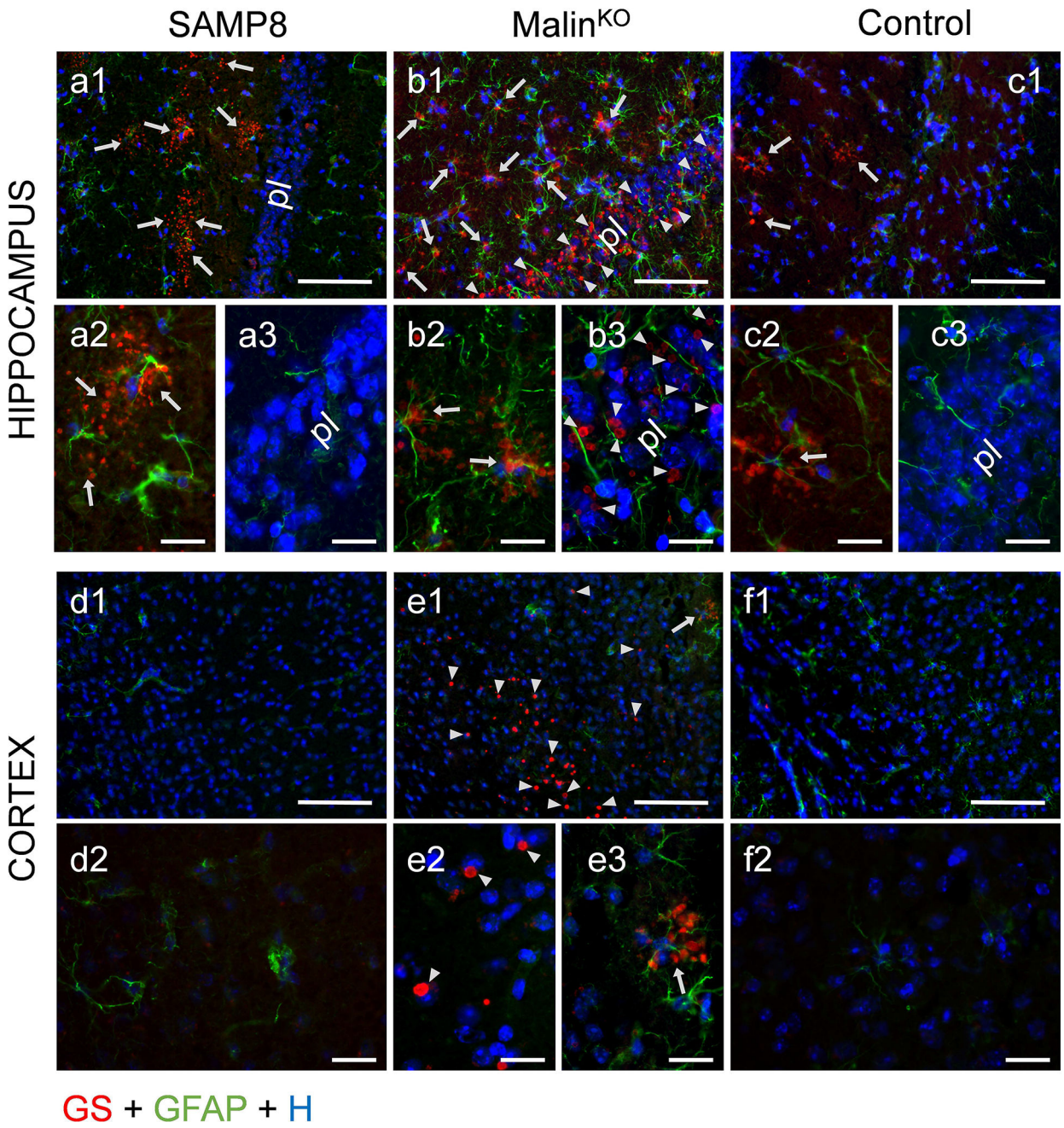


**Figure 1. PGBs associated with astrocytes in SAMP8, malin$^{KO}$ and control animals**

Representative images of hippocampal and cortical brain sections from SAMP8, malin$^{KO}$ and control mice double immunostained with anti-GS (red) and anti-GFAP (green) antibodies. Hoechst (blue) was used for nuclear staining. Hippocampal brain sections from SAMP8, malin$^{KO}$ mice, and, sporadically, control mice, show clusters of astrocyte-associated CAL granules (arrows in a1, b1 and c1). In some cases, the whole astrocyte involved in the formation of a cluster of CAL granules can be observed (a2, b2 and c2). Malin$^{KO}$ mice also present some non-astrocyte-associated PGBs (arrowheads), located mainly in the pyramidal layer (pl) of the hippocampal CA3 region (b1 and b3). These non-

Author Manuscript Author Manuscript Author Manuscript Author Manuscript

astrocyte-associated PGBs are not detected in SAMP8 or control animals (a3, c3). Cortex brain sections from malin$^{KO}$ mice also contain non-astrocyte-associated PGBs (arrowheads in e1), which are located near to some nuclei (e2), and only a few clusters of CAL granules (e3). The cortex of SAMP8 and control animals do not show PGBs (d1, d2, f1 and f2). Arrows: clusters of astrocyte-associated CAL granules. Arrowheads: non-astrocyte-associated PGBs. Scale bar a1-f1: 100 μm; a2-f2, a3-c3 and e3: 20 μm.

Author Manuscript Author Manuscript Author Manuscript Author Manuscript

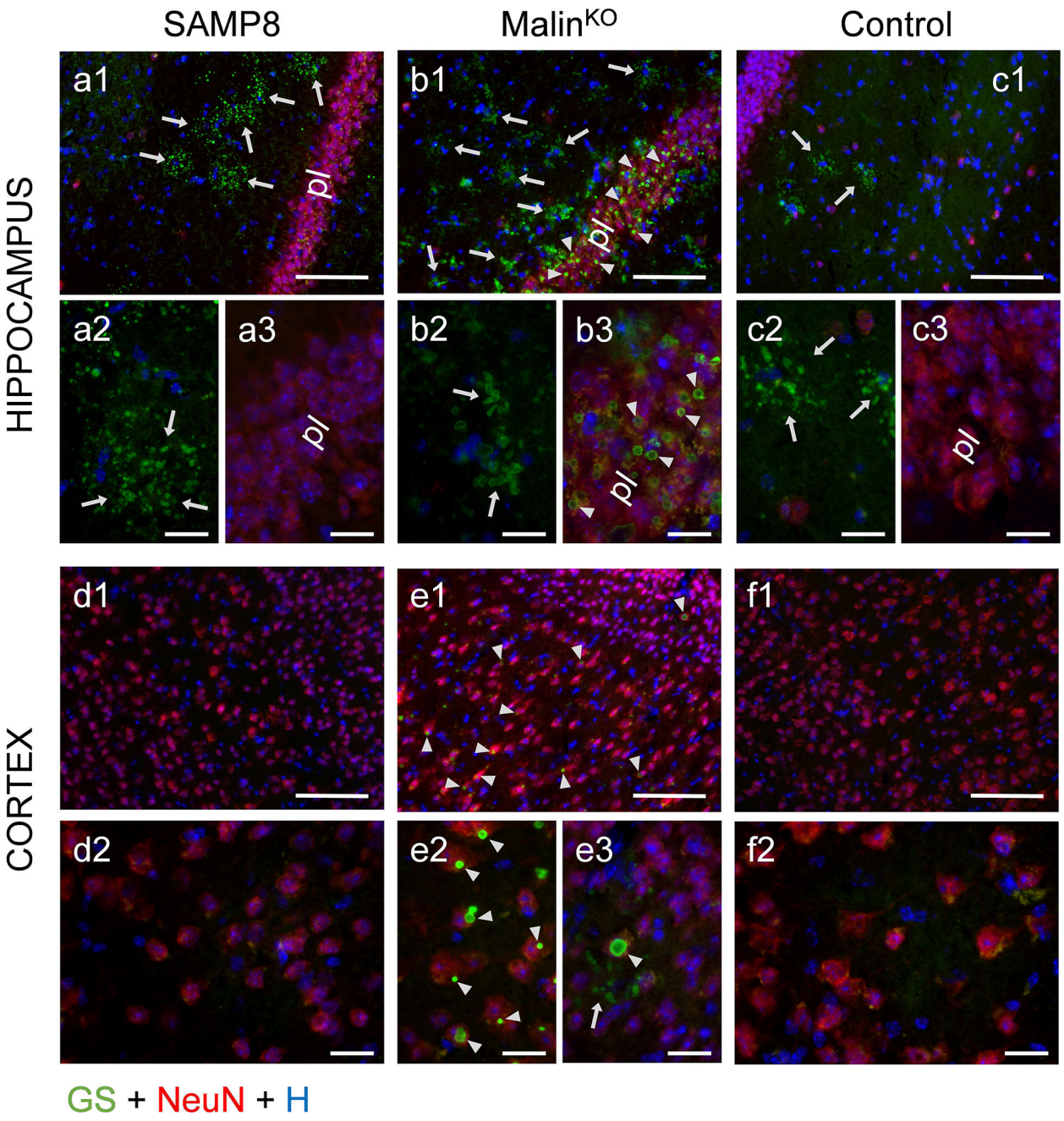


**Figure 2. PGBs associated with neurons in malin$^{KO}$ animals**

Representative images of hippocampal and cortical brain sections from SAMP8, malin$^{KO}$ and control mice double immunostained with anti-GS (green) and NeuN (red) antibodies. Hoechst (blue) was used for nuclear staining. Malin$^{KO}$ mice show neuronal PGBs (arrowheads in b1 and b3) and clusters of CAL granules (arrows in b1 and b2) in the hippocampus. Neuronal PGBs are mainly in the pyramidal layer. Hippocampal sections of SAMP8 mice show CAL granules (a1 and a2). Clustered CAL granules are also observed in control animals (c1 and c2), but in low numbers. Neither SAMP8 or control mice show neuron-associated PGBs in the hippocampus (a3 and c3). Neuron-associated and some non-

Author Manuscript Author Manuscript Author Manuscript Author Manuscript

neuron-associated PGBs can be observed in the cortex of malin$^{KO}$ animals (e1, e2 and e3). No PGBs were observed in the cortex of SAMP8 or control animals (d1, d2, f1 and f2). As neuronal PGBs are exclusive to the malin$^{KO}$ mouse, a model of Lafora disease, and they are found in neurons, they are referred to as neuronal Lafora bodies (nLBs). Arrows: clusters of CAL granules. Arrowheads: nLBs. pl: pyramidal layer of the hippocampus. Scale bar a1-f1: 100 μm; a2-f2, a3-c3 and e3: 20 μm.

Author Manuscript Author Manuscript Author Manuscript Author Manuscript

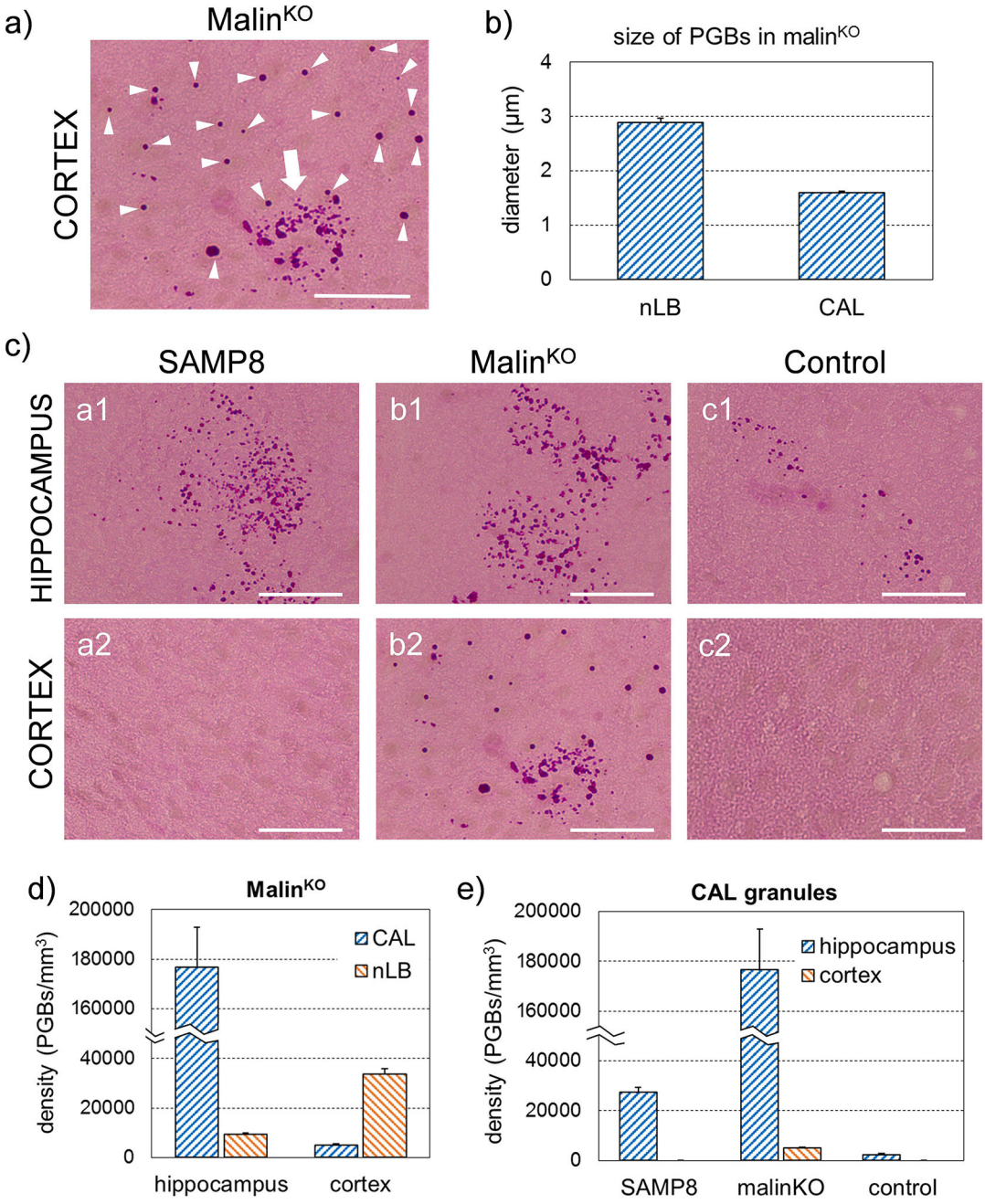


**Figure 3. CAL granules, smaller than nLBs, predominate in the hippocampus while nLBs predominate in the cortex**

(a) Representative image of the cortex of a malin$^{KO}$ mouse immunostained with PAS, in which nLBs (arrowheads) and a cluster of CAL granules (arrow) can be observed. (b) Histogram showing the mean diameter (and SEM) of nLBs and CAL granules in the cortex of malin$^{KO}$ mice. (c) Representative images of the hippocampus and cortex of SAMP8, malin$^{KO}$ and control mice. Clusters of CAL granules can be observed in the hippocampus of all animals. Some clusters of CAL granules are also observed in the cortex of malin$^{KO}$ mice, which also includes nLBs (see detail in image a). (d) Histogram showing the density of CAL granules and nLBs in the hippocampus and cortex of malin$^{KO}$ animals. (e) Histogram

showing the density of CAL granules in the hippocampus and cortex of SAMP8, malin$^{KO}$ and control animals. All histograms express the mean and SEM, and significant differences are detailed in the text. Scale bars: 100 μm.

Author Manuscript Author Manuscript Author Manuscript Author Manuscript

Author Manuscript Author Manuscript Author Manuscript Author Manuscript

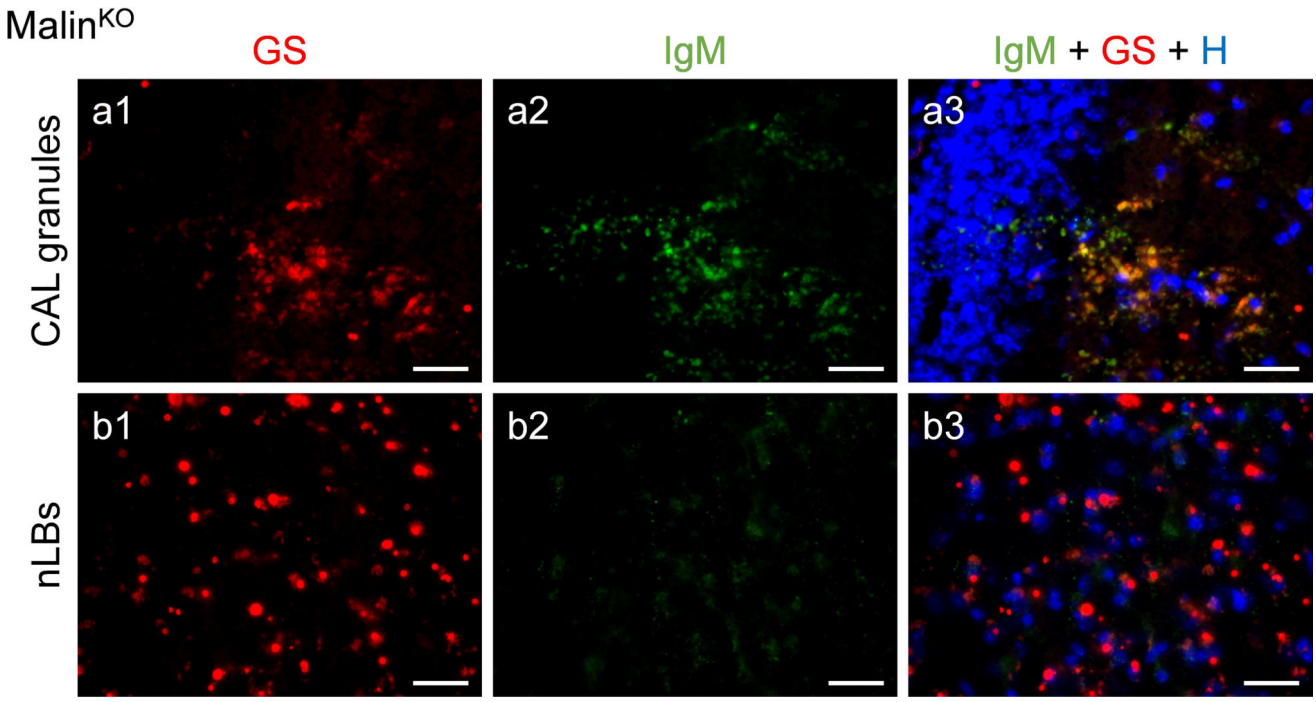


**Figure 4. CAL granules, but not nLBs, contain neo-epitopes**

Representative images of hippocampal (a1–a3) and cortex (b1–b3) regions of malin$^{KO}$ mice double immunostained with anti-GS antibody (red) and IgMs (green). Hoechst (H, blue) was used for nuclear staining. A cluster of CAL granules from the hippocampus is stained with GS (a1) and also with IgMs (a2). Colocalization (yellow to orange) can be observed in the merged image (a3), indicating that CAL granules contain neo-epitopes. PGBs associated with neurons (nLBs) are stained with anti-GS antibody (b1) but not with the IgMs (b2). The absence of colocalization (b3) indicates that nLBs do not contain neo-epitopes. Scale bar: 20 μm.

Author Manuscript Author Manuscript Author Manuscript Author Manuscript

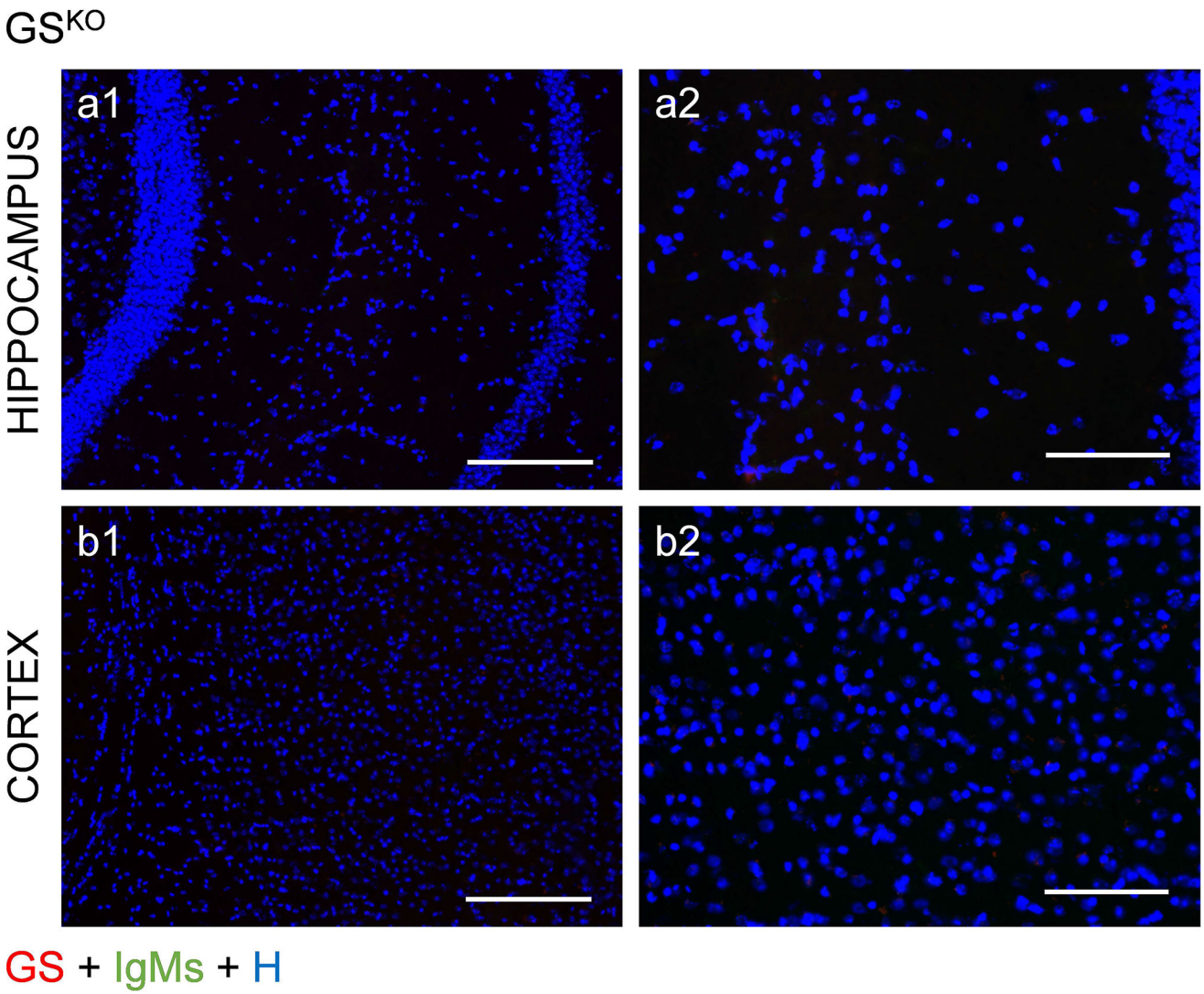


**Figure 5. GS is necessary for the detection of clusters of granules containing neo-epitopes**

Representative images of hippocampal and cerebral cortex regions of $MGS^{KO}$ mice double immunostained with anti-GS antibody (red) and IgMs (green). Hoechst (H, blue) was used for nuclear staining. The absence of clusters of granules containing neo-epitopes indicate that the glycosidic structure of CAL granules is necessary for the presence of these epitopes. Scale bar a1 and b1: 200 μm; a2 and b2: 100 μm.

Author Manuscript Author Manuscript Author Manuscript Author Manuscript

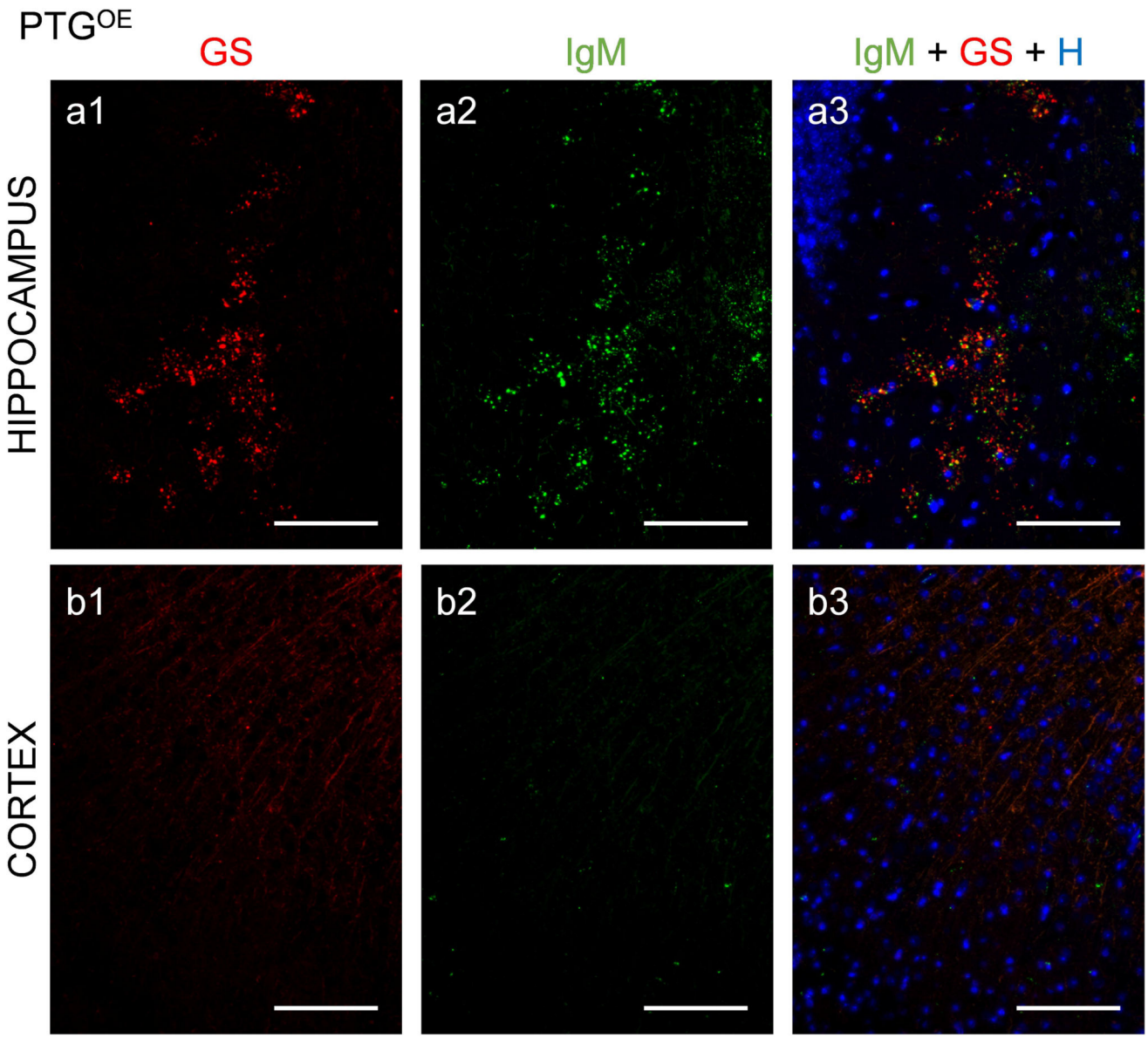


**Figure 6. PTG$^{OE}$ animals present CAL granules but not nLBs**

Representative images of hippocampal and cerebral cortex regions of PTG$^{OE}$ mice double immunostained with anti-GS antibody (red) and IgMs (green). Hoechst (H, blue) was used for nuclear staining. CAL granules stained with anti-GS antibody (a1) and IgMs (a2) can be observed in the hippocampus, and they are also visible in the merged image (a3). These animals, however, do not present nLBs, as can be seen in cortex images stained with anti-GS antibody (b1) and IgMs (b2) or in the merged image (b3). Scale bar: 100 μm.

Author Manuscript Author Manuscript Author Manuscript Author Manuscript

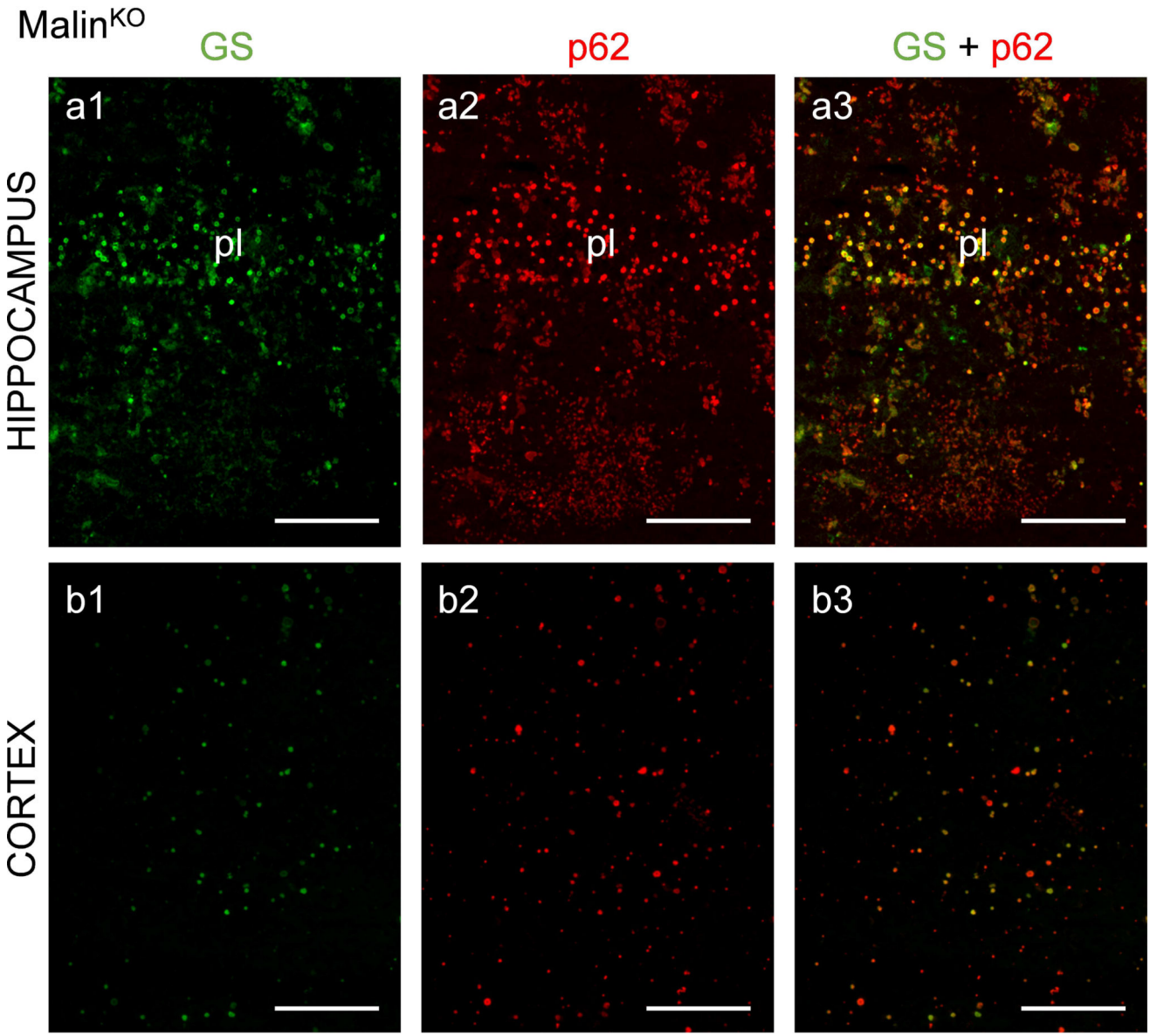


**Figure 7. Autophagy marker p62 is present in both CAL granules and nLBs**

Representative images of hippocampal and cerebral cortex regions of malin$^{KO}$ mice double immunostained with anti-GS (green) and anti-p62 (red) antibodies. Hoechst (H, blue) was used for nuclear staining. CAL granules and nLBs stained with both anti-GS (a1) and anti-p62 (a2) antibodies can be observed in the hippocampus. nLBs, also stained with anti-GS (b1) and anti-p62 (b2) antibodies, can also be seen in the cortices of the animals. Both types of granules can be also appreciated in the merged images (a3, b3). These results indicate that both types of PGB contain the p62 autophagy marker. pl: pyramidal layer of the hippocampus. Scale bar: 100 μm.

Author Manuscript Author Manuscript Author Manuscript Author Manuscript



**Table I**

Type and features of PGBs present in each strain or transgenic mouse model

| | Type of PGBs | Formed in | Presentation | Density[1] in Cx (PGBs/mm$^3$) | Density[1] in Hc (PGBs/mm$^3$) | Size[1] in Cx (μm) | Neoepitopes |
|---|---|---|---|---|---|---|---|
| **Malin$^{KO}$** | nLBs | neurons | isolated | 33671.06 (±2217.18) | 9324.92 (±592.69) | 2.83 (±0.22) | absent |
| | CAL | astrocytes | clustered | 4936.45 (±594.91) | 176709.32 (±16058.40) | 1.59 (±0.18) | present |
| **C57BL/6** | CAL | astrocytes | clustered | --- | 2388.17 (±428.63) | --- | present |
| **SAMP8** | CAL | astrocytes | clustered | --- | 27560.24 (±1742.26) | --- | present |
| **PTG$^{OE}$** | CAL | astrocytes | clustered | n.a. | n.a. | n.a. | present |
| **MGS$^{KO}$** | --- | --- | --- | --- | --- | --- | --- |

PGBs: polyglucosan bodies; nLBs: neuronal Lafora bodies; CAL: *corpora amylacea*-like granules; Hp: hippocampus; Cx: cerebral cortex. --- indicates absence of granules. n.a.: data not available.

[1] expressed as mean (± standard error of the mean).

*Glia*. Author manuscript; available in PMC 2019 October 01.